



HAL
open science

Chronic recording of cortical activity underlying vocalization in awake minipigs

Marie Palma, Mehrdad Khoshnevis, Marie Lion, Cyril Zenga, Samy Kefs, Florian Fallegger, Giuseppe Schiavone, Isabelle Gabelle Flandin, Stéphanie Lacour, Blaise Yvert

► To cite this version:

Marie Palma, Mehrdad Khoshnevis, Marie Lion, Cyril Zenga, Samy Kefs, et al.. Chronic recording of cortical activity underlying vocalization in awake minipigs. *Journal of Neuroscience Methods*, 2022, 366, pp.109427. 10.1016/j.jneumeth.2021.109427. hal-04837581

HAL Id: hal-04837581

<https://hal.science/hal-04837581v1>

Submitted on 19 Dec 2024

HAL is a multi-disciplinary open access archive for the deposit and dissemination of scientific research documents, whether they are published or not. The documents may come from teaching and research institutions in France or abroad, or from public or private research centers.

L'archive ouverte pluridisciplinaire **HAL**, est destinée au dépôt et à la diffusion de documents scientifiques de niveau recherche, publiés ou non, émanant des établissements d'enseignement et de recherche français ou étrangers, des laboratoires publics ou privés.



Distributed under a Creative Commons Attribution - NonCommercial 4.0 International License

1 Chronic recording of cortical activity underlying vocalization in awake 2 minipigs

3 Marie Palma^{1*}, Mehrdad Khoshnevis^{1*}, Marie Lion¹, Cyril Zenga¹, Samy Kefs², Florian Fallegger³,
4 Giuseppe Schiavone³, Isabelle Gabelle Flandin², Stéphanie Lacour³, Blaise Yvert¹

- 5 1. Inserm, Univ Grenoble Alpes, Grenoble Institute of Neurosciences U1216, Grenoble, France
6 2. CHU Grenoble Alpes, Clinique Universitaire de Cancérologie-Radiothérapie, Grenoble, France
7 3. Ecole Polytechnique Fédérale de Lausanne (EPFL), Laboratory for Soft Bioelectronic
8 Interfaces, Geneva, Switzerland

9
10 * Authors contributed equally to this work

11 12 Corresponding author:

13 Blaise Yvert, PhD.
14 INSERM and Univ Grenoble Alpes
15 Grenoble Institute of Neuroscience U1216
16 2280 rue de la piscine
17 38610 Gières, France
18 blaise.yvert@inserm.fr

19 **Highlights**

- 20 - Minipigs can be implanted safely over motor cortex before frontal sinuses develop
21 - Production of grunts activates the motor/premotor region around vocal onset
22 - This vocal-evoked potential lasted for the duration of the vocalization

23 **Abstract**

24 **Background:** Investigating brain dynamics underlying vocal production in animals is a powerful way
25 to inform on the neural bases of human speech. In particular, brain networks underlying vocal
26 production in non-human primates show striking similarities with the human speech production
27 network. However, despite increasing findings also in birds and more recently in rodents, the extent
28 to which the primate vocal cortical network model generalizes to other non-primate mammals
29 remains unclear. Especially, no domestic species has yet been proposed to investigate vocal brain
30 activity using electrophysiological approaches. **New method:** In the present study, we introduce a
31 novel experimental paradigm to identify the cortical dynamics underlying vocal production in
32 behaving minipigs. A key problem to chronically implant cortical probes in pigs is the presence and
33 growth of frontal sinuses extending caudally to the parietal bone and preventing safe access to
34 neural structures with conventional craniotomy in adult animals. **Results:** Here we first show that
35 implantations of soft ECoG grids can be done safely using conventional craniotomy in minipigs
36 younger than 5 months, a period when sinuses are not yet well developed. Using wireless recordings
37 in behaving animals, we further show activation of the motor and premotor cortex around the onset
38 of vocal production of grunts, the most common vocalization of pigs. **Conclusion:** These results
39 suggest that minipigs, which are very loquacious and social animals, can be a good experimental
40 large animal model to study the cortical bases of vocal production.

41 **Keywords**

42
43 Vocal production, pig, porcine model, motor cortex, neural implant, ECoG
44

45 Introduction

46 Animals communicate through multiple types of acoustic signaling (Chen and Wiens, 2020), and
47 many vertebrates, including birds and marine and terrestrial mammals, have the ability to produce
48 vocalizations that often differ depending on the type of information they want to communicate
49 (Brudzynski, 2010). In primates, two types of vocal behaviors can be distinguished that have been
50 proposed to stem from two different neural pathways (Jürgens, 2002; Hage and Nieder, 2016; Hage,
51 2018; Mooney, 2020): Innate affective and learned volitionally controlled vocalizations. Innate
52 vocalizations are determined genetically and are typically produced automatically by cingulate-
53 subcortical networks in reaction to a stimulus or a situation (such as fear, pain, hunger, or surprise).
54 By contrast, learned vocalizations, characterized by single or sequences of stereotyped calls or more
55 complex modulated sounds, are acquired by experience and volitionally controlled by cortical
56 networks involving motor, premotor and inferior frontal areas (Coudé et al., 2011; Hage et al., 2013;
57 Fukushima et al., 2014; Okubo et al., 2015; Roy et al., 2016; Gavrilov et al., 2017; Loh et al., 2017).
58 Cortical networks have also been shown to be important for vocal learning and temporal patterning
59 in birds and mice (Aronov et al., 2008; Long and Fee, 2008; Okobi et al., 2019; Tschida et al., 2019;
60 Mooney, 2020). Although noticeable variations of anatomical pathways exist between humans and
61 non-human primates (NHPs) that may explain at least in part the unique ability of humans to speak
62 (Rilling et al., 2008), the brain networks underlying vocal production show strong anatomical
63 similarities between humans and NHPs (Petrides et al., 2005; Hage, 2018) and to some extent birds
64 (Chakraborty and Jarvis, 2015). However, until now, very few neurophysiological data highlighting
65 the cortical dynamics underlying vocal production have been reported in animal models other than
66 NHPs, rodents and birds. Especially, no domestic species has yet been proposed to investigate vocal
67 brain activity using electrophysiological approaches.

68 The domestic pig (*sus domesticus*) is a highly social species that produces a large variety of
69 vocalizations in different situations. Several decades ago, (Kiley, 1972) described ungulates
70 vocalizations and their causations. She proposed a classification of adult pig vocalizations and
71 highlighted four principal types of calls (grunts, barks, screams and squeals) and their situations of
72 occurrence. She also described many variations and subcategories, giving an overview of the
73 potential richness of the pig's vocal repertoire. Further ethological studies have later reported the
74 existence of vocal call subcategories such as long grunts (Marchant et al., 2001) or even intermediate
75 call types such as grunt-squeals (Appleby et al., 1999), suggesting that the vocal repertoire of pigs
76 might be more continuous. Recent studies classified vocalizations in ungulate species (Tallet et al.,
77 2013; Garcia et al., 2016) and concluded that a discrete system was adapted, even if there are
78 evidences of gradation between acoustic categories. Beyond these works, a number of studies have
79 been conducted in situations relevant for commercial farming to assess and improve the welfare of
80 pigs (Fraser, 1975; Jensen and Algers, 1984; Jensen and Redbo, 1987; Xin et al., 1989; Weary and
81 Fraser, 1995; Manteuffel et al., 2004; Schön et al., 2004; Whittemore and Kyriazakis, 2006; Moura et
82 al., 2008; da Silva Cordeiro et al., 2013; Illmann et al., 2013). These works have thus improved our
83 understanding of pig vocalizations and how they reflect their mental or physical state. Moreover, pigs
84 are domestic animals that are easier to care for compared to wild species such as NHPs, and have
85 been increasingly attracting attention in the field of neurotechnology and neuroscience (Félix et al.,
86 1999; Jelsing et al., 2006; Lind et al., 2007; Saikali et al., 2010; Van Gompel et al., 2011; Knösche et
87 al., 2015; Paek et al., 2015; Benavides et al., 2017; Bech et al., 2018; Ulyanova et al., 2018; Ernst et
88 al., 2018; Simchick et al., 2019; Vrselja et al., 2019; Cho et al., 2020; Slopsema et al., 2021; Ritter et
89 al., 2021) including cognition (Gielsing et al., 2011). In particular, minipigs have become a purpose
90 bred for research. They are smaller yet physiologically in all other ways similar to agricultural pigs.
91 For research lasting longer than 3 weeks, minipigs are thus preferable both for handling ease and
92 welfare considerations. Furthermore, they have a convenient body size for surgical procedures and
93 given their anatomical similarities to humans, they are often used as preclinical models (Selek et al.,
94 2014; Khoshnevis et al., 2017, 2020; Schiavone et al., 2018; Fallegger et al., 2021).

95 In the present study, we introduce a novel experimental paradigm to identify the cortical dynamics
96 underlying vocal production in behaving minipigs. A key problem to chronically implant neural probes
97 in a pig's brain is the presence and development of frontal sinuses preventing safe access to neural
98 structures with conventional craniotomy in adult animals (Gierthmuehlen et al., 2011; Torres-
99 Martinez et al., 2019). These cavities indeed extend far caudally within the skull of adult animals from
100 the frontal to the parietal bones. Performing a craniotomy in such condition leads to cross the
101 sinuses and thus to make a connection between the implanted zone and the nasal cavity, which
102 ineluctably eventually leads to postoperative infections. Here we first show that implantations of soft
103 ECoG grids can be done using conventional craniotomy in minipigs younger than 5 months, a period
104 when frontal sinuses are not yet well developed. Using wireless recordings in behaving animals, we
105 further show activation of the motor and premotor cortex around the onset of vocal production of
106 grunts, the most common vocalization of pigs.

107

108

109 **Materials and Methods**

110 ***Animals***

111 This study was carried out in Aachener (Carfil, Oud-Turnhout, Belgium) and Göttingen (Ellegaard,
112 Dalmoose, Denmark) minipigs. Eight animals were imaged to determine a surgical procedure allowing
113 chronic implantation of cortical probes, and two animals were implanted with soft implants as
114 described below (one of which broke its implant connector before recordings could be conducted).
115 Experiments were conducted in compliance with European (2010-63-EU) and French (decree 2013-
116 118 of rural code articles R214-87 to R214-126) regulations on animal experiments, following the
117 approval of the local Grenoble ethical committee ComEth C2EA-12 and the French Ministry of
118 Research (APAFIS#5221-2016042816336236.V3). Animals were typically housed in groups with
119 weekly renewed enrichment materials and ad libitum water. Implanted minipigs were also housed
120 most of the time with other congeners. Regular examinations were performed by a veterinarian and
121 animals were socialized to ease human-animal interactions. At the end of this study, the implanted
122 minipig in which we recorded cortical activity was rehabilitated in a pedagogic farm as a retirement.

123 ***Imaging (CT-scan and MRI)***

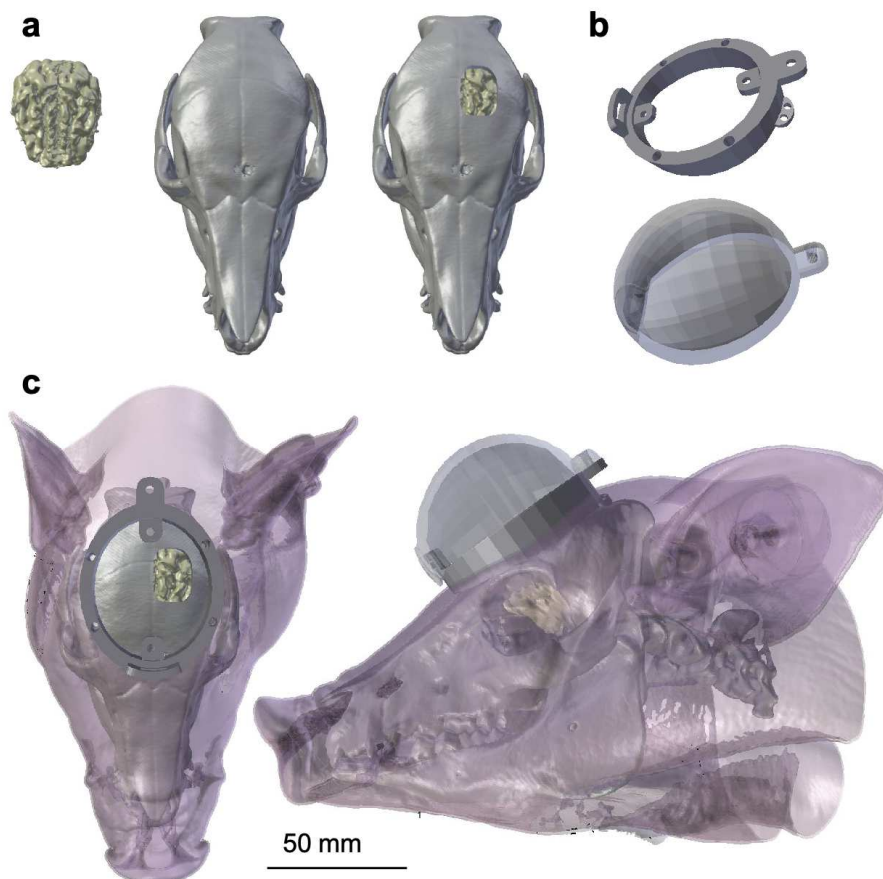
124 In order to overcome the problem of frontal sinuses during the craniotomy, CT-scans were acquired
125 at different ages between 3 and 12 months to assess the development of frontal sinuses. CT images
126 were acquired at the Grenoble Hospital using a GE LightSpeed RT 16 CT Scanner (Helicoidal
127 acquisition, 1.25 mm slice thickness and step) except for the 2 animals aged 5.5 and 12 months, for
128 which they were provided by Ellegaard. CT-scans were used to define the craniotomy area over the
129 skull as proposed previously for NHPs (Chen et al., 2017). For logistical reasons, no CT-scan was
130 performed for one of the implanted animals (CH596), so the CT acquisition of the other implanted
131 animal of similar age and same strain (BA638) was used in this case. For CT imaging, each animal was
132 pre-medicated with an IM injection of 1mg/kg Azaperone (Stresnil®, Elanco, Suresnes, France). After
133 15-20 minutes, an anesthesia was induced by intramuscular (IM) injection of 5mg/kg Tiletamine-
134 Zolazepam (Zoletil® 100, Virbac, Carros, France). For the two animals that were implanted, a pre-
135 surgical T1-weighted MRI (T1-MDEFT, 1-mm slice thickness, 0.43x0.43 mm² pixels, TE: 4 ms, TR: 2000
136 ms, Flip angle: 20°) was performed under a general anesthesia induced as for CT-scans and then
137 further maintained under Isoflurane (Isoflo®, 2-2.5%).

138 ***Surgery preparation using 3D modeling and printing***

139 Chronically implanted devices in large animals require protection components to secure fragile
140 electronics and connectors from hits, bites or even breaking. To do so, customizable pieces adapted

141 to the animal anatomy were developed using 3D modeling following a procedure inspired by a
142 previously proposed method for NHPs (Chen et al., 2017). The CT images were imported in the
143 InVesalius software (2007-2017, Center for Information Technology Renato Archer) and segmented
144 to obtain a 3D model of the skull. The MR images were processed with 3D Slicer software
145 (<http://www.slicer.org>) (Fedorov et al., 2012) to segment the brain and visualize the cortical gyrus
146 and sulcus anatomy before implantation in order to make accurate anatomic assessment of the
147 motor cortex for surgical planning. The 3D models obtained by CT-scan and MRI were then combined
148 using the Blender software (<https://www.blender.org/>) to model the full minipig's head. Based on
149 this reconstruction, the coordinates of the craniotomy were planned according to the motor cortex
150 location to access the implantation area (Figure 1a).

151 A custom metallic oval chamber (60x50mm) was further designed to be screwed on the skull during
152 the implantation surgery (Figure 1b, top). This chamber was adjusted to the minipig anatomy to
153 closely fit its skull surface. Its role was to cover and protect the craniotomy area and house the
154 connector of the implant. To ensure good resistance against possible damages, this chamber was 3D
155 printed in biocompatible TA6V titanium (X3D, Lyon France). To close this chamber, a thick hood
156 3D printed in transparent resin using a Form 2 printer (Formlabs, Sommerville, USA) (Figure 1b,
157 bottom). This piece could be easily removed by the experimenter for each recording session to
158 connect the recording devices.



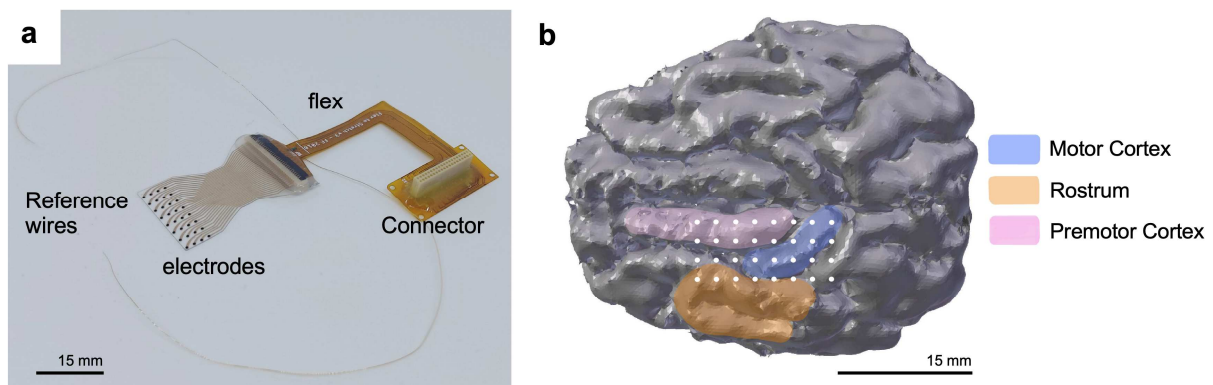
159
160 **Figure 1. Surgery planning using 3D modeling.** (a) 3D modeling of a minipig's brain based on T1 MR images,
161 and skull based on a CT-Scan. Right: The craniotomy area could be planned before the surgery to target the
162 motor cortex. (b) Titanium chamber to be screwed on the skull (top) and plastic protective cap (bottom). (c) Full
163 head reconstruction where the skin is also represented together with the chamber and the protective hood
164 closing the chamber. Scale in (c) also applies to (a).

165

166 **Implantation surgery**

167 In the present study, two Aachener female minipigs (BA638 aged 4 months and CH596 aged 4.5
168 months) were chronically implanted with a soft electrocorticographic (EcoG) array made of a silicone
169 (polydimethylsiloxane, PDMS) substrate and housing 32 electrode contacts arranged in a 4x8 layout
170 covering 5x15 mm² and routed to a 36-pin Omnetics connector (Figure 2a) together with a reference
171 and a ground wires (PFA coated gold wires, Science Products). This implant was designed to fit the
172 left motor cortex of the animal (Figure 2b) based on previous anatomical studies (Sauleau et al.,
173 2009; Saikali et al., 2010; Benavides et al., 2017). The detailed properties of this implant as well as
174 preliminary results have been reported elsewhere (Fallegger et al., 2021). Animal BA638 broke his
175 cap and the implant tail before recordings could be performed. The geometry of the cap was then
176 modified to avoid this problem with animal CH596 for which chronic recordings could be obtained
177 and reported below. One recording of this animal corresponds to the one reported in (Fallegger et
178 al., 2021).

179



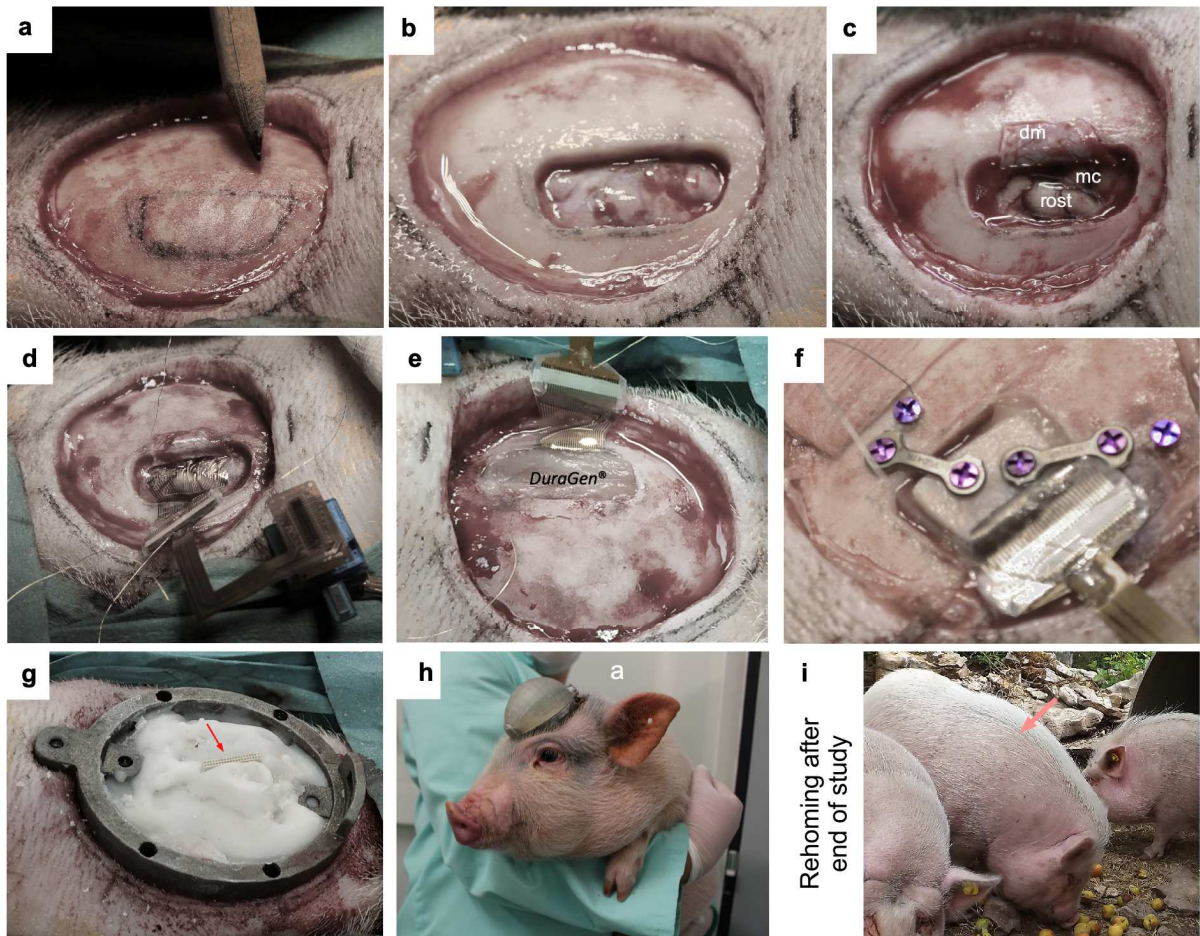
180

181 **Figure 2. Soft cortical implant used in this study.** (a) General view of the soft implant housing 32 electrodes
182 routed to an Omnetics® connector (Fallegger et al., 2021). (b) Reconstruction of the cortical surface of the
183 implanted animal CH596 showing the eventual position of the electrodes with respect to the motor and premotor
184 areas (Sauleau et al., 2009; Saikali et al., 2010; Benavides et al., 2017).

185 For the surgical implantation, the animal was initially premedicated and anesthetized using IM
186 Stresnil and Zoletil as for CT and MRI imaging (see above). A trimmer was then used to shave the hair
187 over the head from the eyes up to the back of the ear's roots. Then, the pig was placed in a
188 stereotaxic frame (David KOPF Instrument, USA) over a warming blanket to prevent the peri-
189 operative hypothermia. The pig's head was typically fixed by the ear bars with a slight extension of
190 the head. To continue the general anesthesia, sedation was maintained by a continuous inhalation of
191 isoflurane 2% (Selek et al., 2014; Khoshnevis et al., 2017, 2020; Torres-Martinez et al., 2019).
192 Ketoprofen (3 mg/kg, Ketofen® CEVA) was administered IM to better maintain the anesthesia and
193 improve postoperative analgesia. Before beginning the surgery, the skin incision site and extensive
194 area surrounding it were disinfected by wiping skin with betadine scrub 4% and dermal 10%
195 immediately prior to draping. Cardio-respiratory functions were monitored throughout the surgical
196 procedure. Local analgesia was provided by subcutaneous (SC) injections of lidocaine (xylocaine
197 adrenaline) before incising the skin according to the later position of titanium chamber on the skull.

198 An oval incision was done to remove a part of the scalp (Figure 3a). Using a periosteal elevator, the
199 periosteum was retracted gently to the edge of the skull. The entire exposed area of the skull was
200 well dried and cleaned. The craniotomy area was drawn over the left hemisphere of the skull based
201 on the skull anatomical cues such as bregma, occipital crest, temporal crest, and
202 central tubercle of nuchal crest and according to the position of the motor cortex relative to bregma.
203 In practice, the craniotomy extended roughly from 5 mm posterior to 20 mm anterior to bregma and
204 from 2 mm to 18 mm lateral of the midline. The skull was drilled gently with electric surgical drill

205 (Medtronic). When the full thickness craniotomy has been reached, the bone flap was lifted away
 206 from the skull (Figure 3b). After exposing the dura mater, its surface was dried and cleaned to ensure
 207 no further bleeding. Then the dura mater was cut with micro-dissecting scissors to reach the
 208 implantation area on the brain surface (Figure 3c).



209
 210

211 **Figure 3. Chronic implantation of a soft ECoG implant.** (a) Oval opening of the skin and drawing of the
 212 craniotomy based on CT-scan. (b) Craniotomy after removal of portion of the skull (bone flap). (c) Craniotomy
 213 with opened dura mater (dm) over motor cortex (mc) and rostrum (rost). (d) Positioning of the soft implant. (e)
 214 duraplasty by Duragen®. (f) closure of the craniotomy with bone flap. (g) Titanium chamber screwed on the
 215 skull and cemented connector (arrow). (h) Implanted animal several days after surgery with protective cap
 216 closing the chamber. (i) Explanted animal CH596 (middle pointed by arrow) rehomed with congeners in a farm
 217 after ending its investigation. All panels refer to animal CH596 except panel f corresponding to animal BA638
 218 (the same approach was used for CH596 but no picture of this step was taken during the surgery).

219

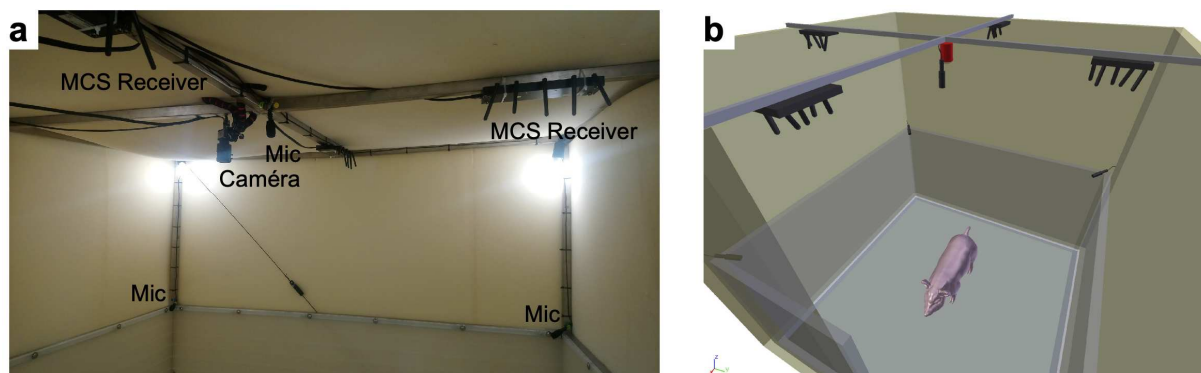
220 The soft implant was positioned to cover the premotor and motor cortices (Figure 3d), slightly
 221 extending caudally to the postcentral gyrus. After the implantation, unilateral duraplasty was
 222 performed using an onlay, suture-free, 3-dimensional-collagen matrix graft (*DuraGen*®, Integra
 223 LifeSciences) (Figure 3e). To close the craniotomy, the bone flap was slightly thinned and placed back
 224 on the Duragen, and then fixed on the surrounding skull using titanium strips and screws. The
 225 titanium chamber was then fixed on the skull using self-drilling titanium screws. The reference wires
 226 were rolled around and laced on supplementary bone screws inserted next to the craniotomy area
 227 (Figure 3f). Then, the interior space of the chamber was filled with bone cement (CMW1 +
 228 Gentamycin®, DEPUY) to seal the craniotomy and surrounding area and to fix the Omnetics
 229 connector (Figure 3g, arrow). At the end of the surgery, the chamber was closed by the 3D printed

230 hood to protect the implant connector when the animal was replaced in the housing pen (Figure 3h).
231 After surgery, the animal was monitored in a recovery room, pain relief was anticipated with an
232 injection of Ketoprofen (3mg/kg). Prophylactic antibiotics (Kesium® CEVA) and anti-inflammatory
233 agent (Metacam® Boehringer Ingelheim) were administered for 7 days postoperative. At the end of
234 the study, the explanted animal was rehomed in a farm through the GRAAL society
235 (<https://www.graal-defenseanimale.org/>) (Figure 3i). Two subsequent animals (one Göttingen and
236 one Aachener) were implanted following a similar procedure with other arrays, for which we only
237 report thereafter the anatomical evolution of their skull after explantation (Figure 6).

238 ***Simultaneous electrophysiological, audio and video recordings***

239 Neural activity was recorded using the wireless W2100 system (MultichannelSystems, Reutlingen,
240 Germany). A 2m x 2m x 2m recording pen was built and sound-attenuated using several layers of
241 acoustic foam (Figure 4).

242



243 **Figure 4. Experimental setup for synchronous recording of vocal and cortical data in minipigs.** (a) Roof of the
244 recording pen with the recording setup. (b) 3D schematics of the recording pen with a behaving animal.
245

246 Four wireless receivers were fixed on the roof of the pen and connected to 2 recording interface
247 boards located outside the pen. Five microphones (Pro45, Audio-Technica Inc, USA) were positioned
248 in the pen, one at each corner 1m from the floor and one on the ceiling in the center of the pen,
249 where a camera (UI-3140CP-C-HQ Rev.2, IDS Imaging, Obersulm, Germany) was also positioned to
250 monitor the animal behavior. During a typical experimental session, the protecting hood was
251 detached and a wireless HS32 headstage (MultichannelSystems, Reutlingen, Germany) was
252 connected to the implant. Then, the animal could be let to move and behave freely in the pen under
253 the supervision of an experimenter. However, in order to avoid that the animal damages the
254 headstage against the floor or the walls, an experimenter placed her on her laps or in her arms. This
255 physical contact was also a way to arouse more vocalizations. Synchronous cortical, audio and video
256 data acquisitions were performed with the MCS experimenter software. Neural data was acquired at
257 a 20-kHz sampling rate after 1-5000 Hz bandpass filtering and 16-bits AD conversion at the headstage
258 level. Audio data was acquired at 20kHz after amplification by a sound card (OctoMic II, RME-Audio,
259 Haimhausen, Germany). Video was acquired at 50Hz, synchronized with the neural and audio data.

260 ***Neural data processing***

261 Cortical data was band-pass filtered between 1 and 10 Hz and evoked potentials were computed by
262 averaging single trials locked to the onset of vocalizations (detected by thresholding the audio signal
263 and classified manually) and correcting the baseline with respect to the [-3s, -2 s] interval preceding
264 the vocalization onset. We then evaluated the reproducibility of the averaged evoked potential by
265 building a distribution of bootstrap averages (Yvert et al., 2002). If N vocalizations were recorded, N
266 trials were drawn with replacement from the original set of N trials, and averaged and baseline-
267 corrected. This procedure was repeated 1000 times. To further assess the statistical significance of
268 vocalization-induced cortical activations, we used the following approach. A 60-second rest period

269 void of vocal production was considered and used to select N resting trials, which were in turn
270 averaged and baseline corrected. The standard deviations corresponding to both the vocalization and
271 the resting averages were also computed and a Welch t-test was performed to compare both
272 distributions at every time point of the average potential. A threshold was set at 0.05 and individual
273 electrode values at all time points for which the p-value of the Welch test was below this threshold
274 were considered to correspond to statistically significant activity. This procedure was thus further
275 retained to build spatiotemporal maps of cortical activity using our previously developed NeuroMap
276 software (Abdoun et al., 2011) (freely available at
277 <https://sites.google.com/site/neuromapsoftware/>).

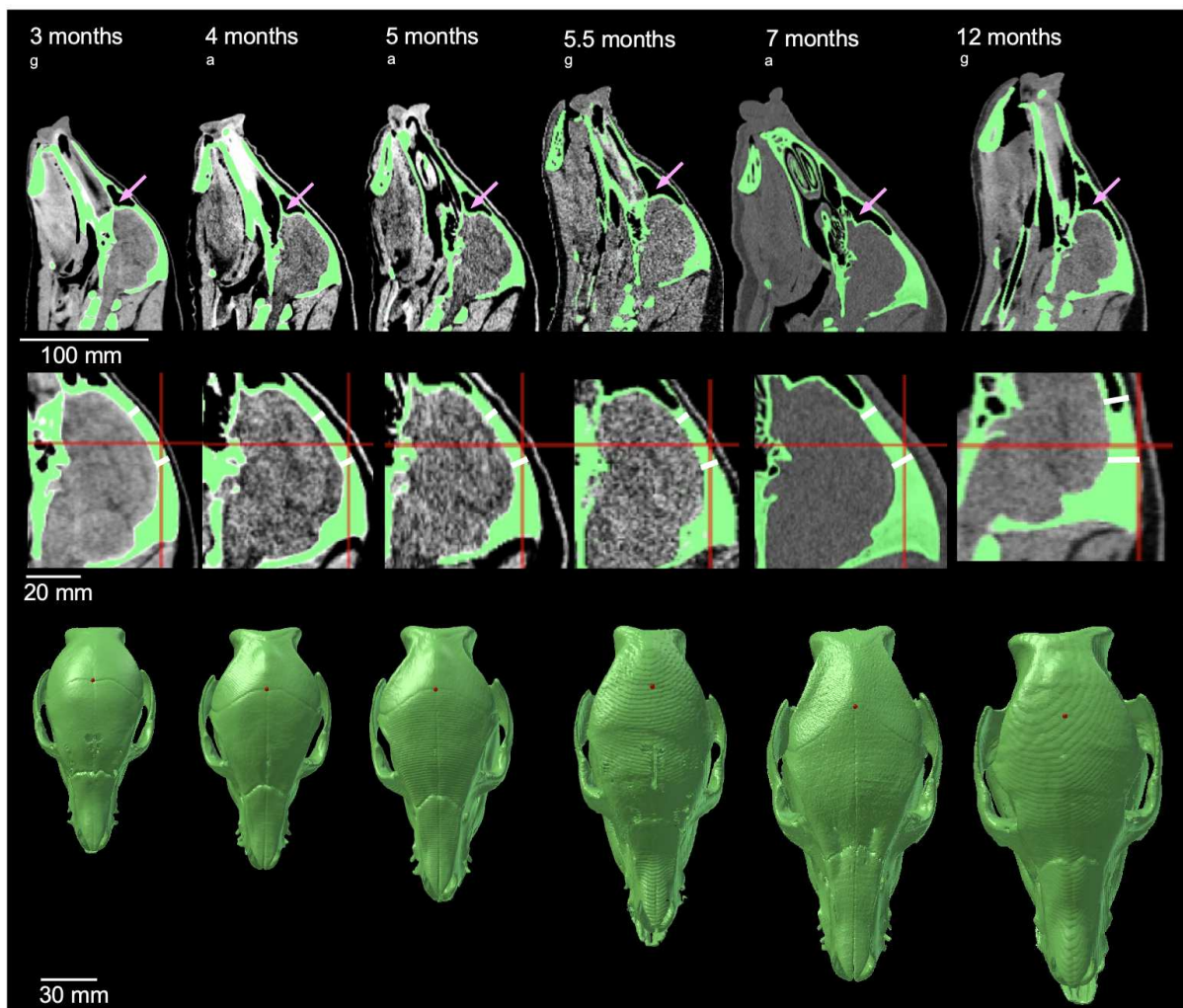
278

279 Results

280 *Normal development of frontal sinuses*

281 From the several CT acquisitions made at different ages of control Aachener and Göttingen minipigs,
282 it was observed that before 5 months of age, the sinuses have not yet extended too caudally and the
283 motor cortex could be accessible through a conventional craniotomy (Figure 5). Thanks to this
284 acquired information, the minipigs were implanted at 4-4.5 months of age using a craniotomy
285 exposing the motor cortex and part of the rostrum and prefrontal cortex (see Figure 3).

286

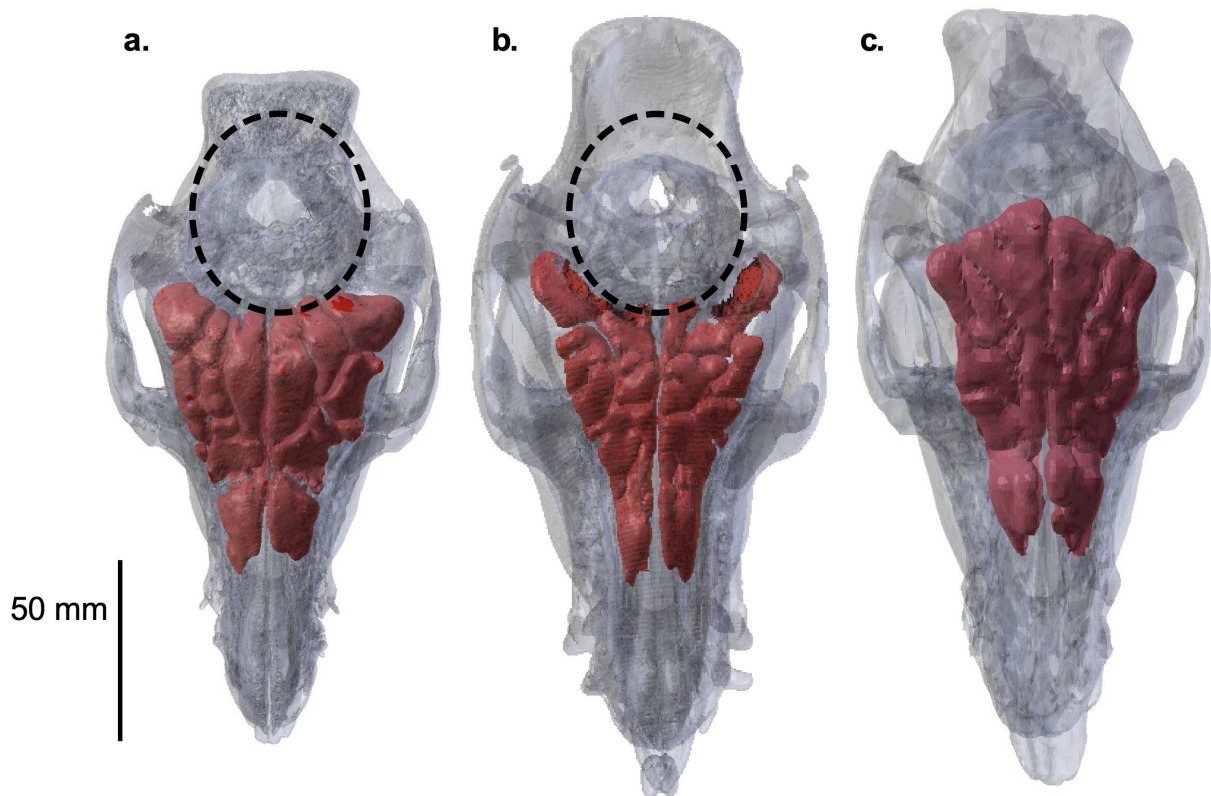


287 **Figure 5. Development of frontal sinuses in minipigs between 3 and 12 months of age.** Top row: Mid-sagittal
288 CT images of the whole head at various ages. The skull is colored in green and the frontal sinus is indicated by
289

290 the pink arrow. Middle row: close-up view of the brain area, with a representation of a typical target craniotomy
291 over the motor cortex (white marks). The red cross indicates Bregma. Bottom row: Top view of the skull with
292 Bregma indicated by a red dot. a=Aachener minipigs, g=Göttingen minipigs.

293 **Development of frontal sinuses in case of chronic implantation**

294 We then analyzed the volumes of the sinuses of two other animals that had been implanted with
295 other types of implants but the same chamber and craniotomy and for which CT-scans were obtained
296 after their implants had been removed, and compared them to that of a control non-implanted
297 animal. As illustrated in Figure 6, we found that in the implanted animals, the sinuses did evolve
298 caudally but around the zone of the skull that was exposed to position the chamber. In particular, the
299 sinuses did not develop in the zone of the craniotomy, so that no infection could be induced by their
300 evolution after the implantation.



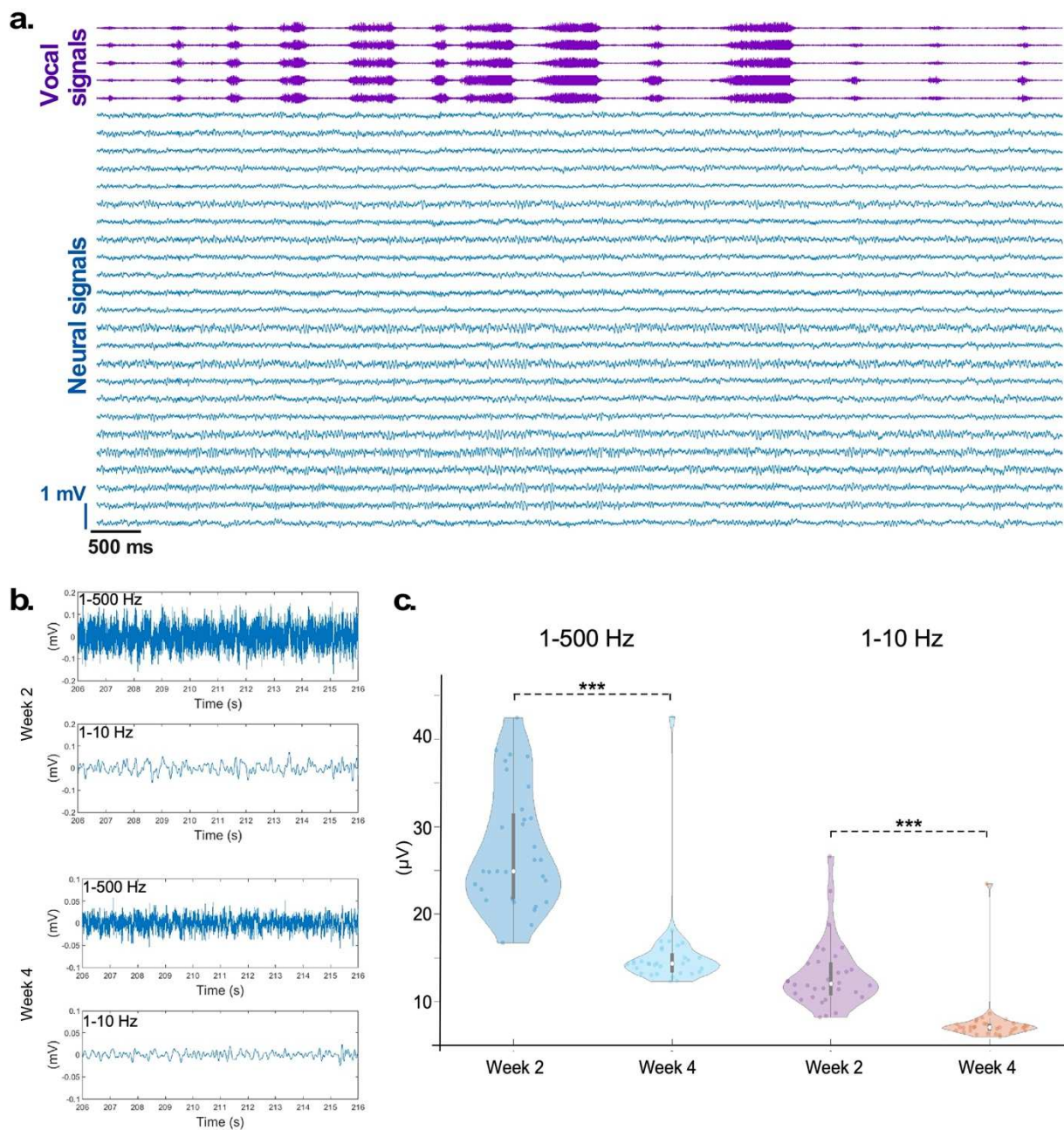
301 **Figure 6. Development of frontal sinuses in minipigs following an implantation.** The volume of the frontal
302 sinuses is reconstructed in red from CT-scans acquired in two implanted animals after they have been explanted
303 and in one control animal. The position of the chamber is indicated by a dashed line for the implanted animals.
304 a) 7.5-month-old Göttingen minipig 3 months after implantation. b) 12-month-old Aachener minipig 7 month
305 after implantation. c) Control not implanted 12-month-old Göttingen minipig.
306

307

308 **Vocal production activates premotor and motor areas**

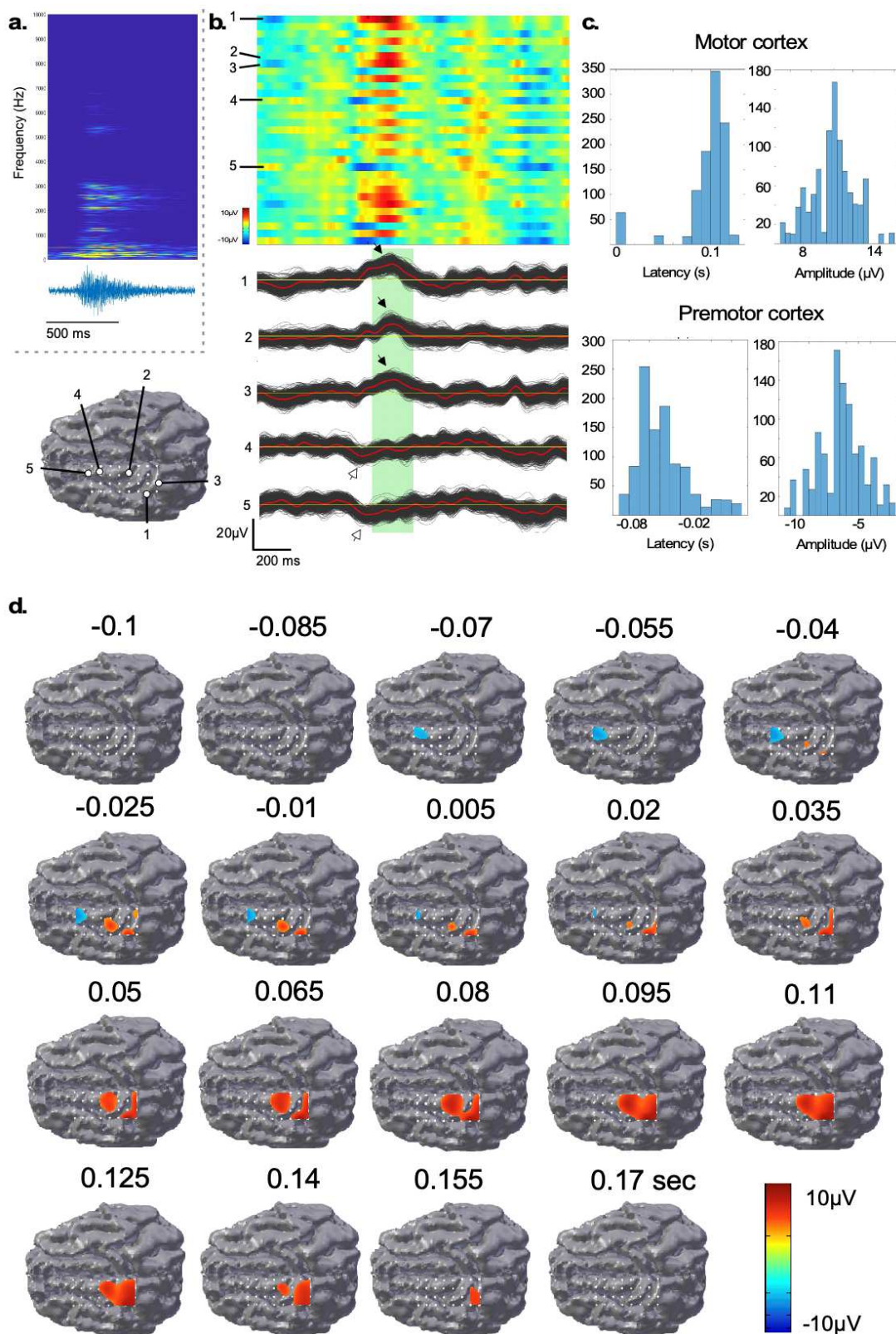
309 Two recordings were performed 2 and 4 weeks after implantation, respectively, an example of raw
310 data being shown in Figure 7a. We observed a decrease of the baseline noise level of the recording
311 between both sessions (1-500 Hz: $p=0.9 \cdot 10^{-5}$; 1-10 Hz: $p=1.2 \cdot 10^{-5}$, Wilcoxon rank sum tests) (Figure
312 7b&c). Minipigs produced different types of vocalizations, most of which were grunts. We thus
313 focused on this particular vocalization (Figure 8a). In the first session, we observed statistically
314 significant cortical activity on several electrodes of the array (Figure 8b&c), with an initial anterior
315 activity of $-6 \mu\text{V}$ peaking on average 41 ms before vocal onset over the premotor cortex followed by a
316 more caudal activity over the motor cortex peaking on average 120 ms after vocal onset with an
317 amplitude of $11 \mu\text{V}$. The overall spatiotemporal dynamics of this vocal production related activity is

318 illustrated in Figure 7d on the cortical anatomy. In the second session, no premotor activity was
 319 observed but we found statistically significant cortical activity over the motor cortex consistent with
 320 that observed in the first session. This activity peaked on average 157 ms after vocal onset with an
 321 amplitude of 5.4 μV . A comparison of this motor activity between both sessions is presented in
 322 Figure 9. The cortical responses over the motor region were visible at the single trial level, especially
 323 in the second session (Figure 9a). These motor potentials lasted for the duration of the vocalization
 324 (Figure 9b), which were on average longer in the second session compared to the first (385 ms versus
 325 210 ms). In particular longer grunts elicited longer evoked potentials (Figure 9a). Across both
 326 sessions, the spatial extent of this activity was very similar (Figure 9c), and tended to follow more
 327 closely the cruciate gyrus housing the primary motor cortex in session 2 compared to session 1,
 328 possibly indicating that the implant tended to better match the cortical folding over time post-
 329 implantation.



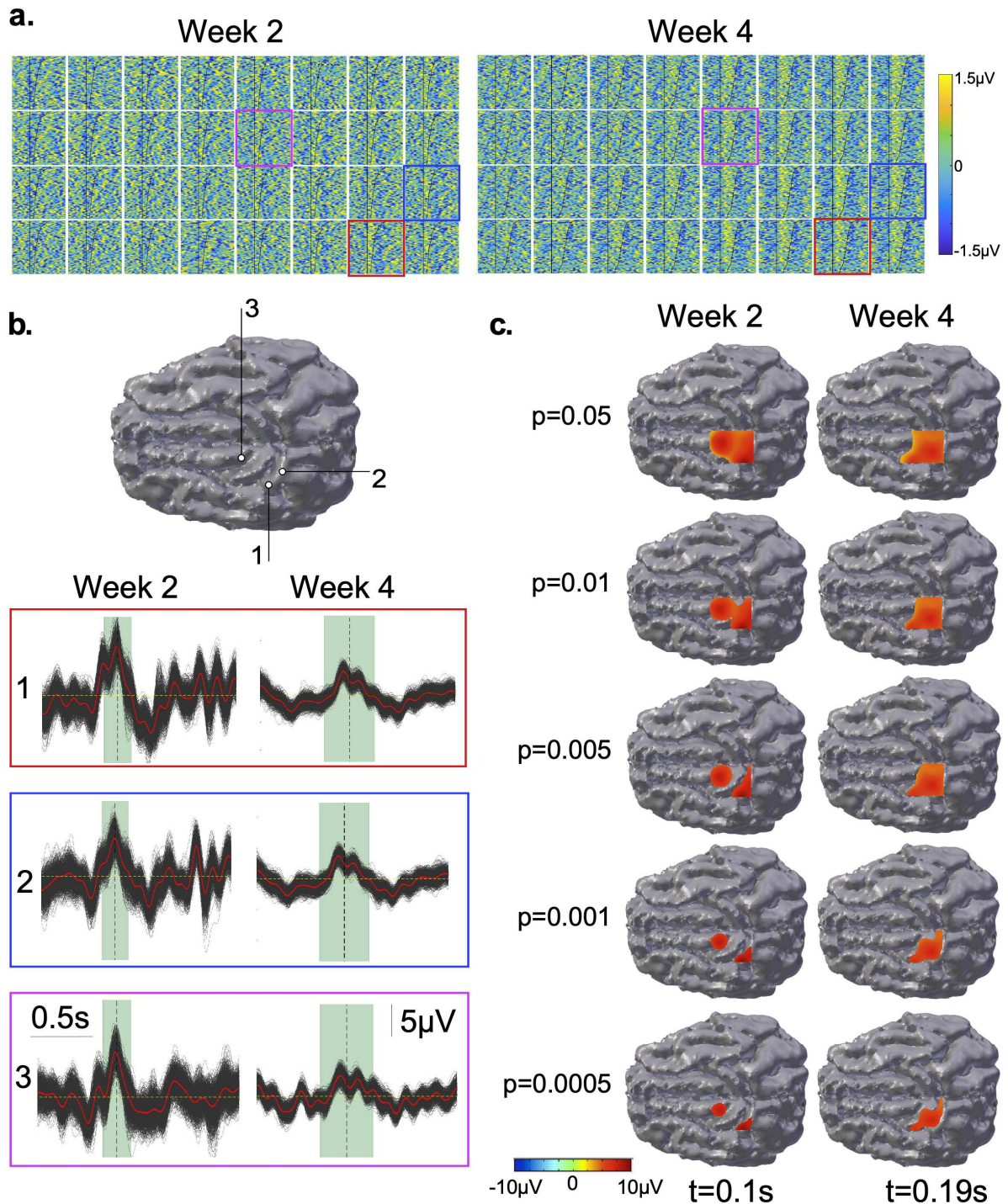
330
 331 **Figure 7. Evolution of baseline noise amplitude between 2 and 4 weeks after implantation.** (a) Example of 10
 332 seconds of simultaneous audio and raw neural data recorded in animal CH596. (b) Example of raw signal for
 333 one electrode in the 1-500 Hz and 1-10 Hz frequency bands recorded at 2 and 4 weeks post implantation. (c)

334 quantification of baseline noise (*computed as the standard deviation of the signal over 60 seconds*) for all the
 335 electrodes. These signals were obtained while the animal was awake and correspond to the baseline signal used
 336 to threshold the activity maps in Figure 8 and 9 (see methods).



337
 338 **Figure 8. Cortical responses to vocal production of grunts in minipig CH596 over the motor/premotor region.**
 339 (a) Example of spectrogram and raw audio signal of a grunt vocalization. (b) Averaged evoked potentials ($n =$
 340 75 grunts) color scaled across the array and for 5 electrodes of interest. Red curve= original average; black

341 curves: bootstrap averages. The average vocal duration is represented by the green interval, the horizontal
 342 yellow line represents $0 \mu\text{V}$. (c) Distributions of the latencies and amplitudes of the motor (black arrows in b)
 343 and premotor (white arrows in b) responses obtained from the bootstrap averages. (d) Time-varying spatial
 344 maps of statistically significant vocal-triggered cortical potential over the brain anatomy.



345
 346 **Figure 9. Comparison of cortical responses to vocal production of grunts between two recording sessions 2**
 347 **and 4 weeks after implantation, respectively.** (a) Color-coded vocal-evoked potentials for all vocal occurrences
 348 (1 line per vocalization) and all electrodes displayed according to the 4x8 grid as in Figure 2b. The vertical
 349 black line indicates vocal onsets and the black curve on its right indicates the vocal offsets. Trials are sorted by
 350 vocal durations, the shortest corresponding to the lowest line of each color plot. (b) Bootstrap (black) and
 351 original (red) averages for 3 electrodes located over the motor region (framed in a). The green area indicates
 352 the mean vocal duration for each session. The yellow dashed line indicates $0 \mu\text{V}$. (c) spatial extent of the motor
 353 cortical activity assessed at different statistical levels of the Welch test (see Methods) for each session. These

354 *maps correspond to the activity at the time of the middle of the vocalization as indicated by the vertical dashed*
355 *lines in panel b.*

356

357

358 **Discussion**

359 The primary goal of this paper was to describe an experimental approach enabling chronic recordings
360 of cortical activity underlying vocal production in behaving minipigs. Planning implantation of cortical
361 electrode arrays in young animals was found to be key to make possible a craniotomy over the motor
362 cortex and even more frontal areas, without the usual risk of infection encountered when such
363 surgery is performed in adult animals with well-developed frontal sinuses. Based on CT images, we
364 found that sinuses cover the anterior part of the brain at around 5 months of age, so that performing
365 implantation by this age avoids crossing the meninges cavities and thus opening a direct route of
366 infection from the nasal cavity to the brain. Interestingly, no such route further develops over the
367 months following the implantation. As shown in Figure 6, the proposed surgical procedure indeed
368 modifies the course of development of the sinuses so that they do not invade the part of the skull
369 bone over which the skin and the periosteum have been removed. The sinuses continue to grow
370 caudally after the implantation but skirt around this area (Figure 6b). As a result, no infection
371 developed at the level of the craniotomy and the brain tissue over the months after surgery.

372 Working with minipigs with chronic cortical implants requires practical precautions to ensure the
373 sustainability of chronic recordings. In particular, these animals like to explore and interact with their
374 environment with their head. This implies a reliable protection of the zone of extracutaneous
375 connectors necessary for external connections with the recording system. The suitable solution we
376 found was the fixation of a titanium chamber over the skull closed by a solid removable plastic hood
377 (Figure 1 & 3). It was important that the hood did not present any poking asperities that the animal
378 could use against its pen environment to apply a lever force that would break its attachment to the
379 chamber and expose the implant connector. Because the scalp was removed over the area of the
380 chamber, regular care was needed to maintain the external ridge of the chamber clean and avoid
381 local infections. Importantly, a recovery of full skull coverage by the skin was observed after the
382 chamber was removed when explanting the animal. This regrowth process took 1-2 months
383 depending on the individual, and ensured that the animal could then be rehomed in a natural
384 farming environment (Figure 3i).

385 The paradigm proposed in this paper opens the way to use minipigs as a new chronic experimental
386 model for neuroscience research and particularly to study the cortical bases of vocalization in a large
387 non-primate mammal species. Minipigs indeed represent interesting subjects for this field, because
388 they are very loquacious animals, producing many vocalizations spontaneously, especially when in
389 groups or when interacting with humans. Moreover, they are domestic animals with advanced
390 cognitive capabilities (Broom et al., 2009; Gieling et al., 2011) that can be handled easily by humans
391 without the need of coercive relationships, which is another asset for investigating behavioral
392 paradigms.

393 Previous findings in NHPs, birds, and mice, have been increasingly describing the involvement of
394 cortical structures in the production of vocalizations, especially when volitionally produced. In
395 primates, this cortical network involves the primary motor, premotor SMA, and inferior frontal
396 regions (Gemba et al., 1995, 1997, 1999; Romanski et al., 2005; Coudé et al., 2011; Hage and Nieder,
397 2013; Plakke et al., 2013; Roy et al., 2016; Gavrillov et al., 2017), and its neuroanatomical organization
398 shares large similarities between NHPs and humans (Loh et al., 2017; Nieder and Mooney, 2020). Yet,
399 the extent to which it can generalize to other mammals remains unknown. Here, in the animal
400 presented in this study to illustrate the proposed paradigm, we found that the production of grunts,
401 the most common vocalization of pigs, elicited an activation of the motor and premotor region,

402 starting about 40 ms before vocal onset over the premotor cortex and then involving the motor
403 cortex. The activity over the motor cortex was consistent across both recording sessions and its
404 duration was found to follow the duration of the vocalization (Figure 9a, right). This observation thus
405 suggests that the motor cortex is engaged during vocal production in minipigs. Here, we did not train
406 the animal in any particular way to volitionally produce vocalizations. Vocalizations were rather
407 produced spontaneously while interacting with the experimenter. The fact that a cortical activity was
408 observed could be due to the fact that the animal was on the laps or in the arms of the experimenter,
409 and that vocalizations could thus have been produced volitionally. Future work will be required to
410 highlight this aspect in more details in freely moving animals and also to identify more extensively
411 the cortical network underlying vocal production in pigs and in particular to determine whether it
412 may share similarities with the frontal network previously highlighted in primates.

413

414 **Acknowledgements**

415 This work was supported by the French National Research Agency under Grant Agreement No. ANR-
416 16-CE19-0005-01 (Neuromedde), by the European Union's Horizon 2020 Research and Innovation
417 Programme under Grant Agreements No. 732032 (BrainCom), No. 696656 (GrapheneCore1), No.
418 785219 (GrapheneCore2), No 881603 (GrapheneCore3), with financial support by the Bertarelli
419 Foundation, the Wyss Center for bio- and Neuroengineering (Grant No. W015-2016), the European
420 Union's Horizon 2020 Research and Innovation Programme under the Marie Skłodowska-Curie grant
421 agreement no. 665667, and the SNSF National Center of Competence in Research (NCCR) in Robotics.
422 The authors are grateful to the Carfil and Ellegaard companies for providing CT scan data, and to the
423 Clinattec preclinical team for animal housing and care. The authors would like to thank the staff at the
424 Neural Microsystems Platform of the Wyss Center for Bio and Neuroengineering in Geneva,
425 Switzerland for their help with the fabrication processes. They also thank P. Roelfsema and X. Chen
426 for helpful advice on surgery.

427

428 **Conflict of Interest**

429 FF. and S.P.L. hold various patents in relation with the present work and are cofounders of Neurosoft
430 Bioelectronics SA.

431

432 **Author contributions**

433 **Marie Palma:** Methodology, Software, Validation, Formal analysis, Investigation (surgeries, in vivo
434 recordings), Writing original draft, Visualization; **Mehrdad Koshnevis:** Methodology, Validation,
435 Investigation (surgeries), Writing original draft; **Marie Lion:** Methodology, Software, Validation,
436 Formal analysis; **Cyril Zenga:** Investigation (surgeries, in vivo recordings); **Samy Kefs:** Investigation
437 (CT-Scans); **Florian Fallegger:** Methodology and Resources (soft implants), Manuscript review and
438 editing; **Giuseppe Schiavone:** Methodology and Resources (soft implants); **Isabelle Gabelle Flandin:**
439 Supervision and Investigation (CT-Scans); **Stéphanie Lacour:** Supervision and funding acquisition (soft
440 implants); **Blaise Yvert:** Conceptualization, Methodology, Software, Validation, Investigation
441 (surgeries, in vivo recordings), Writing original draft, Visualization, Supervision, Project
442 administration, Funding acquisition.

443

444 **References**

- 445 Abdoun O, Joucla S, Mazzocco C, Yvert B (2011) NeuroMap: A Spline-Based Interactive Open-Source
446 Software for Spatiotemporal Mapping of 2D and 3D MEA Data. *Front Neuroinform* 4:119
447 Available at:
448 [http://www.frontiersin.org/Journal/Abstract.aspx?s=752&name=neuroinformatics&ART_DOI=1](http://www.frontiersin.org/Journal/Abstract.aspx?s=752&name=neuroinformatics&ART_DOI=10.3389/fninf.2010.00119)
449 [0.3389/fninf.2010.00119](http://www.frontiersin.org/Journal/Abstract.aspx?s=752&name=neuroinformatics&ART_DOI=10.3389/fninf.2010.00119).
- 450 Appleby MC, Weary DM, Taylor AA, Illmann G (1999) Vocal communication in pigs: Who are nursing
451 piglets screaming at? *Ethology* 105:881–892.
- 452 Aronov D, Andalman AS, Fee MS (2008) A Specialized Forebrain Circuit for Vocal Babbling in the
453 Juvenile Songbird. *Science* 320:630–634.
- 454 Bech J, Glud AN, Sangill R, Petersen M, Frandsen J, Orlowski D, West MJ, Pedersen M, Sørensen JCH,
455 Dyrby TB, Bjarkam CR (2018) The porcine corticospinal decussation: A combined neuronal
456 tracing and tractography study. *Brain Res Bull* 142:253–262 Available at:
457 <https://doi.org/10.1016/j.brainresbull.2018.08.004>.
- 458 Benavides FD, Santamaria AJ, Bodoukhin N, Guada LG, Solano JP, Guest JD (2017) Characterization of
459 Motor and Somatosensory Evoked Potentials in the Yucatan Micropig Using Transcranial and
460 Epidural Stimulation. *J Neurotrauma* 34:2595–2608.
- 461 Broom DM, Sena H, Moynihan KL (2009) Pigs learn what a mirror image represents and use it to
462 obtain information. *Anim Behav* 78:1037–1041.
- 463 Brudzynski S (2010) *Handbook of Mammalian Vocalization* (Brudzynski S, ed). Oxford: Academic
464 Press.
- 465 Chakraborty M, Jarvis ED (2015) Brain evolution by brain pathway duplication. *Philos Trans R Soc B*
466 *Biol Sci*.
- 467 Chen X, Pospel JK, Wacongne C, van Ham AF, Klink PC, Roelfsema PR (2017) 3D printing and modelling
468 of customized implants and surgical guides for non-human primates. *J Neurosci Methods*
469 286:38–55 Available at: <http://dx.doi.org/10.1016/j.jneumeth.2017.05.013>.
- 470 Chen Z, Wiens JJ (2020) The origins of acoustic communication in vertebrates. *Nat Commun* 11:1–8
471 Available at: <http://dx.doi.org/10.1038/s41467-020-14356-3>.
- 472 Cho S, Min HK, In MH, Jo HJ (2020) Multivariate pattern classification on BOLD activation pattern
473 induced by deep brain stimulation in motor, associative, and limbic brain networks. *Sci Rep*
474 10:1–12 Available at: <http://dx.doi.org/10.1038/s41598-020-64547-7>.
- 475 Coudé G, Ferrari PF, Rodà F, Maranesi M, Borelli E, Veroni V, Monti F, Rozzi S, Fogassi L (2011)
476 Neurons controlling voluntary vocalization in the macaque ventral premotor cortex. *PLoS One*
477 6:1–10.
- 478 da Silva Cordeiro AF, de Alencar Nääs I, Oliveira SRM, Violaro F, de Almeida ACM, Neves DP (2013)
479 Understanding vocalization might help to assess stressful conditions in piglets. *Animals* 3:923–
480 934.
- 481 Ernst L, Darschnik S, Roos J, González-Gómez M, Beemelmans C, Beemelmans C, Engelhardt M,
482 Meyer G, Wahle P (2018) Fast prenatal development of the NPY neuron system in the
483 neocortex of the European wild boar, *Sus scrofa*. *Brain Struct Funct* 223:3855–3873 Available at:
484 <http://dx.doi.org/10.1007/s00429-018-1725-y>.
- 485 Fallegger F, Schiavone G, Pirondini E, Wagner FB, Vachicouras N, Serex L, Zegarek G, May A,
486 Constanthin P, Palma M, Khoshnevis M, Van Roost D, Yvert B, Courtine G, Schaller K, Bloch J,
487 Lacour SP (2021) MRI-Compatible and Conformal Electrographic Grids for Translational

488 Research. *Adv Sci* 2003761:1–9.

489 Fedorov A, Beichel R, Kalpathy-Cramer J, Finet J, Fillion-Robin JC, Pujol S, Bauer C, Jennings D,
490 Fennessy F, Sonka M, Buatti J, Aylward S, Miller J V., Pieper S, Kikinis R (2012) 3D Slicer as an
491 image computing platform for the Quantitative Imaging Network. *Magn Reson Imaging*
492 30:1323–1341.

493 Félix B, Léger ME, Albe-Fessard D, Marcilloux JC, Rampin O, Laplace JP, Duclos A, Fort F, Gougis S,
494 Costa M, Duclos N (1999) Stereotaxic atlas of the pig brain. *Brain Res Bull* 49:1–138.

495 Fraser D (1975) Vocalizations of isolated piglets. I. Sources of variation and relationships among
496 measures. *Appl Anim Ethol* 1:387–394.

497 Fukushima M, Saunders RC, Fujii N, Averbeck BB, Mishkin M (2014) Modeling vocalization with ECoG
498 cortical activity recorded during vocal production in the macaque monkey. 2014 36th Annu Int
499 Conf IEEE Eng Med Biol Soc EMBC 2014:6794–6797.

500 Garcia M, Gingras B, Bowling DL, Herbst CT, Boeckle M, Locatelli Y, Fitch WT (2016) Structural
501 Classification of Wild Boar (*Sus scrofa*) Vocalizations. *Ethology* 122:329–342.

502 Gavrilov N, Hage SR, Nieder A (2017) Functional Specialization of the Primate Frontal Lobe during
503 Cognitive Control of Vocalizations. *Cell Rep* 21:2393–2406 Available at:
504 <https://doi.org/10.1016/j.celrep.2017.10.107>.

505 Gemba H, Kyuhou S, Matsuzaki R, Amino Y (1999) Cortical field potentials associated with audio-
506 initiated vocalization in monkeys. *Neurosci Lett* 272:49–52.

507 Gemba H, Miki N, Kazuo S (1995) Cortical field potentials preceding vocalization and influences of
508 cerebellar hemispherectomy upon them in monkeys. *Brain Res* 697:143–151.

509 Gemba H, Miki N, Sasaki K (1997) Cortical field potentials preceding vocalization in monkeys. *Acta*
510 *Oto-Laryngologica, Suppl* 6489:96–98.

511 Gieling ET, Nordquist RE, van der Staay FJ (2011) Assessing learning and memory in pigs. *Anim Cogn*
512 14:151–173.

513 Gierthmuehlen M, Ball T, Henle C, Wang X, Rickert J, Raab M, Freiman T, Stieglitz T, Kaminsky J (2011)
514 Evaluation of μ ECoG electrode arrays in the minipig: Experimental procedure and neurosurgical
515 approach. *J Neurosci Methods* 202:77–86 Available at:
516 <http://dx.doi.org/10.1016/j.jneumeth.2011.08.021>.

517 Hage SR (2018) Dual neural network model of speech and language evolution: new insights on
518 flexibility of vocal production systems and involvement of frontal cortex. *Curr Opin Behav Sci*
519 21:80–87 Available at: <https://doi.org/10.1016/j.cobeha.2018.02.010>.

520 Hage SR, Gavrilov N, Nieder A (2013) Cognitive control of distinct vocalizations in rhesus monkeys. *J*
521 *Cogn Neurosci*.

522 Hage SR, Nieder A (2013) Single neurons in monkey prefrontal cortex encode volitional initiation of
523 vocalizations. *Nat Commun* 4:1–11 Available at: <http://dx.doi.org/10.1038/ncomms3409>.

524 Hage SR, Nieder A (2016) Dual Neural Network Model for the Evolution of Speech and Language.
525 *Trends Neurosci*.

526 Illmann G, Hammerschmidt K, Špinka M, Tallet C (2013) Calling by domestic piglets during simulated
527 crushing and isolation: A signal of need? *PLoS One* 8:1–9.

528 Jelsing J, Hay-Schmidt A, Dyrby T, Hemmingsen R, Uylings HBM, Pakkenberg B (2006) The prefrontal
529 cortex in the Göttingen minipig brain defined by neural projection criteria and cytoarchitecture.

530 Brain Res Bull 70:322–336.

531 Jensen P, Algers B (1984) An ethogram of piglet vocalizations during suckling. *Appl Anim Ethol*
532 11:237–248.

533 Jensen P, Redbo I (1987) Behaviour during nest leaving in free-ranging domestic pigs. *Appl Anim*
534 *Behav Sci* 18:355–362.

535 Jürgens U (2002) Neural pathways underlying vocal control. *Neurosci Biobehav Rev* 26:235–258
536 Available at:
537 [http://www.ncbi.nlm.nih.gov/entrez/query.fcgi?cmd=Retrieve&db=PubMed&dopt=Citation&lis](http://www.ncbi.nlm.nih.gov/entrez/query.fcgi?cmd=Retrieve&db=PubMed&dopt=Citation&list_uids=11856561)
538 [t_uids=11856561](http://www.ncbi.nlm.nih.gov/entrez/query.fcgi?cmd=Retrieve&db=PubMed&dopt=Citation&list_uids=11856561).

539 Khoshnevis M, Carozzo C, Bonnefont-Rebeix C, Belluco S, Leveneur O, Chuzel T, Pillet-Michelland E,
540 Dreyfus M, Roger T, Berger F, Ponce F (2017) Development of induced glioblastoma by
541 implantation of a human xenograft in Yucatan minipig as a large animal model. *J Neurosci*
542 *Methods* 282:61–68.

543 Khoshnevis M, Carozzo C, Brown R, Bardiès M, Bonnefont-Rebeix C, Belluco S, Nennig C, Marcon L,
544 Tillement O, Gehan H, Louis C, Zahi I, Buronfosse T, Roger T, Ponce F (2020) Feasibility of
545 intratumoral 165Holmium siloxane delivery to induced U87 glioblastoma in a large animal
546 model, the Yucatan minipig. *PLoS One* 15:1–19.

547 Kiley M (1972) The Vocalizations of Ungulates , their Causation and Function. *Z Tierpsychol* 31:171–
548 222.

549 Knösche TR, Anwander A, Liptrot M, Dyrby TB (2015) Validation of tractography: Comparison with
550 manganese tracing. *Hum Brain Mapp* 36:4116–4134.

551 Lind NM, Moustgaard A, Jelsing J, Vajta G, Cumming P, Hansen AK (2007) The use of pigs in
552 neuroscience: Modeling brain disorders. *Neurosci Biobehav Rev* 31:728–751.

553 Loh KK, Petrides M, Hopkins WD, Procyk E, Amiez C (2017) Cognitive control of vocalizations in the
554 primate ventrolateral-dorsomedial frontal (VLF-DMF) brain network. *Neurosci Biobehav Rev*
555 82:32–44 Available at: <http://dx.doi.org/10.1016/j.neubiorev.2016.12.001>.

556 Long MA, Fee MS (2008) Using temperature to analyse temporal dynamics in the songbird motor
557 pathway. *Nature* 456:189–194.

558 Manteuffel G, Puppe B, Schön PC (2004) Vocalization of farm animals as a measure of welfare. *Appl*
559 *Anim Behav Sci* 88:163–182.

560 Marchant JN, Whittaker X, Broom DM (2001) Vocalisations of the adult female domestic pig during a
561 standard human approach test and their relationships with behavioural and heart rate
562 measures. *Appl Anim Behav Sci* 72:23–39 Available at:
563 <http://www.ncbi.nlm.nih.gov/pubmed/11259824>.

564 Mooney R (2020) The neurobiology of innate and learned vocalizations in rodents and songbirds.
565 *Curr Opin Neurobiol* 64:24–31.

566 Moura DJ, Silva WT, Naas IA, Tolón YA, Lima KAO, Vale MM (2008) Real time computer stress
567 monitoring of piglets using vocalization analysis. *Comput Electron Agric* 64:11–18.

568 Nieder A, Mooney R (2020) The neurobiology of innate, volitional and learned vocalizations in
569 mammals and birds. *Philos Trans R Soc B Biol Sci* 375.

570 Okobi DE, Banerjee A, Matheson AMM, Phelps SM, Long MA (2019) Motor cortical control of vocal
571 interaction in neotropical singing mice. *Science (80-)* 363:983–988.

- 572 Okubo TS, Mackevicius EL, Payne HL, Lynch GF, Fee MS (2015) Growth and splitting of neural
573 sequences in songbird vocal development. *Nature* 528:352–357 Available at:
574 <http://dx.doi.org/10.1038/nature15741>.
- 575 Paek SB, Min HK, Kim I, Knight EJ, Baek JJ, Bieber AJ, Lee KH, Chang SY (2015) Frequency-dependent
576 functional neuromodulatory effects on the motor network by ventral lateral thalamic deep
577 brain stimulation in swine. *Neuroimage* 105:181–188.
- 578 Petrides M, Cadoret G, Mackey S (2005) Orofacial somatomotor responses in the macaque monkey
579 homologue of Broca’s area. *Nature* 435:1235–1238.
- 580 Plakke B, Diltz MD, Romanski LM (2013) Coding of vocalizations by single neurons in ventrolateral
581 prefrontal cortex. *Hear Res* 305:135–143 Available at:
582 <http://dx.doi.org/10.1016/j.heares.2013.07.011>.
- 583 Rilling JK, Glasser MF, Preuss TM, Ma X, Zhao T, Hu X, Behrens TEJ (2008) The evolution of the
584 arcuate fasciculus revealed with comparative DTI. *Nat Neurosci* 11:426–428.
- 585 Ritter C, Maier E, Schneeweiß U, Wölk T, Simonnet J, Malkawi S, Eigen L, Tunckol E, Purkart L, Brecht
586 M (2021) An isomorphic three-dimensional cortical model of the pig rostrum. *J Comp Neurol*
587 529:2070–2090.
- 588 Romanski LM, Averbeck BB, Diltz M (2005) Neural representation of vocalizations in the primate
589 ventrolateral prefrontal cortex. *J Neurophysiol* 93:734–747.
- 590 Roy S, Zhao L, Wang X (2016) Distinct Neural Activities in Premotor Cortex during Natural Vocal
591 Behaviors in a New World Primate, the Common Marmoset (*Callithrix jacchus*). *J Neurosci*
592 36:12168–12179 Available at: [http://www.jneurosci.org/cgi/doi/10.1523/JNEUROSCI.1646-](http://www.jneurosci.org/cgi/doi/10.1523/JNEUROSCI.1646-16.2016)
593 [16.2016](http://www.jneurosci.org/cgi/doi/10.1523/JNEUROSCI.1646-16.2016).
- 594 Saikali S, Meurice P, Sauleau P, Eliat PA, Bellaud P, Randuineau G, Vérin M, Malbert CH (2010) A
595 three-dimensional digital segmented and deformable brain atlas of the domestic pig. *J Neurosci*
596 *Methods* 192:102–109.
- 597 Sauleau P, Lapouble E, Val-Laillet D, Malbert CH (2009) The pig model in brain imaging and
598 neurosurgery. *Animal* 3:1138–1151 Available at:
599 <http://dx.doi.org/10.1017/S1751731109004649>.
- 600 Schiavone G, Wagner F, Fallegger F, Kang X, Vachicouras N, Barra B, Capogrosso M, Bloch J, Courtine
601 G, Lacour SP (2018) Long-term functionality of a soft electrode array for epidural spinal cord
602 stimulation in a minipig model. In: 2018 40th Annual International Conference of the IEEE
603 Engineering in Medicine and Biology Society (EMBC), pp 1432–1435.
- 604 Schön PC, Puppe B, Manteuffel G (2004) Automated recording of stress vocalisations as a tool to
605 document impaired welfare in pigs. *Anim Welf* 13:105–110.
- 606 Selek L, Seigneuret E, Nogue G, Wion D, Nissou MF, Salon C, Seurin MJ, Carozzo C, Ponce F, Roger T,
607 Berger F (2014) Imaging and histological characterization of a human brain xenograft in pig: the
608 first induced glioma model in a large animal. *J Neurosci Methods* 221:159–165 Available at:
609 <http://www.ncbi.nlm.nih.gov/pubmed/24126047> [Accessed March 28, 2014].
- 610 Simchick G, Shen A, Campbell B, Park HJ, West FD, Zhao Q (2019) Pig Brains Have Homologous
611 Resting-State Networks with Human Brains. *Brain Connect* 9:566–579.
- 612 Slopsema JP, Canna A, Uchenik M, Lehto LJ, Krieg J, Wilmerding L, Koski DM, Kobayashi N, Dao J,
613 Blumenfeld M, Filip P, Min HK, Mangia S, Johnson MD, Michaeli S (2021) Orientation-selective
614 and directional deep brain stimulation in swine assessed by functional MRI at 3T. *Neuroimage*

615 224:117357 Available at: <https://doi.org/10.1016/j.neuroimage.2020.117357>.

616 Tallet C, Linhart P, Policht R, Hammerschmidt K, Šimeček P, Kratinova P, Špinka M (2013) Encoding of
617 situations in the vocal repertoire of piglets (*Sus scrofa*): a comparison of discrete and graded
618 classifications. *PLoS One* 8:e71841 Available at:
619 <http://www.pubmedcentral.nih.gov/articlerender.fcgi?artid=3742501&tool=pmcentrez&render>
620 [type=abstract](http://www.pubmedcentral.nih.gov/articlerender.fcgi?artid=3742501&tool=pmcentrez&render) [Accessed April 22, 2014].

621 Torres-Martinez N, Cretallaz C, Ratel D, Mailley P, Gaude C, Costecalde T, Hebert C, Bergonzo P,
622 Scorsone E, Mazellier J-P, Divoux J-L, Sauter-Starace F (2019) Evaluation of chronically
623 implanted subdural boron doped diamond/CNT recording electrodes in miniature swine brain.
624 *Bioelectrochemistry* 129:79–89 Available at:
625 <http://www.sciencedirect.com/science/article/pii/S156753941930012X>.

626 Tschida K, Michael V, Takatoh J, Han BX, Zhao S, Sakurai K, Mooney R, Wang F (2019) A Specialized
627 Neural Circuit Gates Social Vocalizations in the Mouse. *Neuron* 103:459-472.e4 Available at:
628 <https://doi.org/10.1016/j.neuron.2019.05.025>.

629 Ulyanova A V., Koch PF, Cottone C, Grovola MR, Adam CD, Browne KD, Weber MT, Russo RJ, Gagnon
630 KG, Smith DH, Isaac Chen H, Johnson VE, Kacy Cullen D, Wolf JA (2018) Electrophysiological
631 signature reveals laminar structure of the porcine hippocampus. *eNeuro* 5.

632 Van Gompel JJ, Bower MR, Worrell GA, Stead M, Meier TR, Goerss SJ, Chang SY, Kim I, Meyer FB,
633 Richard Marsh W, Marsh MP, Lee KH (2011) Swine model for translational research of invasive
634 intracranial monitoring. *Epilepsia* 52:49–53.

635 Vrselja Z, Daniele SG, Silbereis J, Talpo F, Morozov YM, Sousa AMM, Tanaka BS, Skarica M, Pletikos M,
636 Kaur N, Zhuang ZW, Liu Z, Alkawadri R, Sinusas AJ, Latham SR, Waxman SG, Sestan N (2019)
637 Restoration of brain circulation and cellular functions hours post-mortem. *Nature* 568:336–343
638 Available at: <http://dx.doi.org/10.1038/s41586-019-1099-1>.

639 Weary DM, Fraser D (1995) Calling by domestic piglets: reliable signals of need? *Anim Behav*
640 50:1047–1055.

641 Whittemore C, Kyriazakis I (2006) Whittemore’s Science and Practice of Pig Production.

642 Xin H, DeShazer JA, Leger DW (1989) Pig vocalizations under selected husbandry practices. *Trans Am*
643 *Soc Agric Eng* 32:2181–2184.

644 Yvert B, Fischer C, Guénot M, Krolak-Salmon P, Isnard J, Pernier J (2002) Simultaneous intracerebral
645 EEG recordings of early auditory thalamic and cortical activity in human. *Eur J Neurosci*
646 16:1146–1150.

647